2009 American Control Conference
Hyatt Regency Riverfront, St. Louis, MO, USA
June 10-12, 2009

Adaptive Disturbance Rejection in the Presence of Uncertain Resonance Mode in Hard Disk Drives

Fan Hong, Chunling Du, Keng Peng Tee, and S. S. Ge

Abstract— **An adaptive on-line scheme is designed to identify the uncertain and time-varying resonance modes in hard disk drive servo systems. Based on the identified results, the uncertain resonance mode is extracted and a peak filter is designed accordingly to provide stronger capability of disturbance suppression. The scheme does not require any extra excitation signal nor additional signal processing for the parameter identification. Compared to conventional method, the rates of learning and error convergence are greatly increased. The scheme can provide good stability margin at high frequency subject to the variation of the resonance frequency and the peak gain. Simulation results show the validity and effectiveness of the proposed scheme.**

Index Terms— **Disturbance rejection, adaptive control, peak filter, hard disk drive.**

I. INTRODUCTION

In hard disk drives (HDDs) technology, the last decade has seen the rapid growth rate of 100% per year in the recording density [1]. The effort is still continuing to push the recording density to beyond 1Tb/in^2. This gives the servo designers a great challenge to stretch out the servo performance by precisely positioning the read/write head on ever narrower tracks.

Various sources which contribute to the positioning accuracy include vibrations caused by mechanical resonance, as well as input and output disturbances. The mechanical resonances, if not being handled properly, will not only worsen the positioning accuracy, but will also lead the closed-loop system into instability. However, the resonances may shift due to the environmental variation especially the temperature changes, the manufacturing/assembly process and material properties [2]. In addition, some resonance modes will be excited by various disturbances especially those output disturbances at high frequencies such as flow-induced vibration (FIV) [3], contact-induced vibration (CIV) [4], etc. Due to the highly uncertain and time-varying manner of these kind of disturbances, the characteristics of the resonance modes being excited will be fast-changing in terms of their peak values and phase. Notch filters have worked very well to suppress the mechanical modes and guarantee the closed-loop stability. Adaptive notch filters have been developed to capture and tolerate shift in resonance frequency [5][6]. However, the servo loop using the notch filters to handle these resonance mode will not have gain attenuation in the sensitivity function at these resonance modes and thus cannot suppress the vibrations caused by the disturbances at these resonance modes.

To achieve higher TPI (track-per-inch) in HDDs, various loop-shaping methods, such as phase stabilized design [7][8], which support lower sensitivity transfer function gain at frequencies with more vibration, have been developed. Motivated by these works, we propose a novel adaptive disturbance rejection scheme which can identify the uncertain and time-varying resonance modes on-line, and provide better disturbance rejection at these modes. The scheme does not require any extra excitation signal nor additional signal processing for the parameter identification except for choosing appropriately the initial identification conditions based on some known information on the uncertain dynamics. It is a simple yet practical method, which is easy for real-time implementation. Compared to conventional methods, the rates of learning and error convergence are greatly increased. Therefore, it can accommodate the fast-changing uncertainties. A peak filter is then designed according to the identified results to provide better disturbance rejection at these uncertain frequencies.

II. PROBLEM FORMULATION

In this section, we present the main idea of the adaptive disturbance rejection scheme proposed in this paper.

The block diagram of the servo control systems for the scheme is shown in Fig. 1, where $C(z)$ is the nominal controller which guarantees the stability for the nominal closed-loop, $\hat{N}(z)$ is used to identify the uncertain dynamics, $C_{pf}(z)$ is the peak filter used to provide disturbance rejection, $P_n(z)$ and $P_u(z)$ denote the nominal plant dynamics and uncertain plant dynamics respectively, $d_o(k)$ and $n(k)$ are used to represent the output disturbance and measurement noise respectively, assuming the input disturbance can be converted into output disturbance, $r(k)$ is the reference signal and $r(k)$=0 for track-following mode.

The objective of designing $\hat{N}(z)$ is to let the measured position error signal (PES) $y_m(k)$ follow the nominal output $y^*(k)$ as closely as possible. The parameters of $\hat{N}(z)$ are tuned on-line using the approximation error $e(k) = y_m(k) - y^*(k)$ under an adaptive law. By doing so, the uncertain resonance modes can be identified, and as soon as the identification is settled down, a peak filter $C_{pf}(z)$ will be designed to replace $\hat{N}(z)$ according to the identified results

This work is supported by A*Star SERC, Singapore (Grant No. 025 101 0036).

F. Hong and C. Du are with Data Storage Institute, Agency for Science, Technology and Research (A*STAR), DSI Building, 5 Engineering Drive 1, Singapore 117608 HONG_Fan@dsi.a-star.edu.sg

K. P. Tee is with Institute for Infocomm Research, A*STAR, Singapore 138632

S. S. Ge is with the Dept. of Electrical & Computer Engineering, National University of Singapore, Singapore 117605

to provide better disturbance rejection at these uncertain modes. Note that both $\hat{N}(z)$ and $C_{pf}(z)$ are augmented in an "add-on" fashion so that the performance of the nominal controller is well-preserved [8] and both of them can be easily enabled or disabled to accommodate the fast-changing uncertainties.

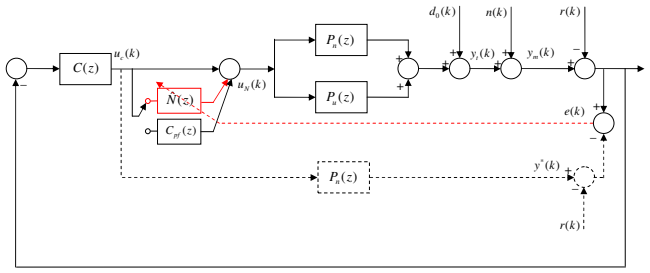

Fig. 1. Block diagram of adaptive resonance rejection scheme.

The mechanical structure of the voice-coil-motor (VCM) model is usually represented by a second order system dominant at a low frequency along with some resonance modes at high frequencies as

$$P_{mech}(s) = K_p \sum_{i=1}^{N_r} \frac{k_i}{s^2 + 2\zeta_i\omega_i s + \omega_i^2} \tag{1}$$

where N_r, k_i, ζ_i, ω_i are the number of resonance mode, the residue of the resonance mode, the damping ratio and natural frequency of the resonance mode respectively, and K_p is the plant gain. The input time delay or dead time e^{-sT_d} is usually modeled by the first-order Pade approximation as $e^{-T_d s} \approx \frac{2-T_d s}{2+T_d s}$. Thus, the full model of the VCM actuator is

$$P_f(s) = K_p\left(\frac{2 - T_d s}{2 + T_d s}\right) \sum_{i=1}^{N_r} \frac{k_i}{s^2 + 2\zeta_i\omega_i s + \omega_i^2} \tag{2}$$

In HDD head positioning servomechanism, the PES signal is sampled into a discrete signal before passing to the digital microprocessor to compute the control signal, which is then converted to a continuous signal by the D/A converter and the hold, and then supplies to the VCM actuator. For a plant $P_f(s)$ preceded by a zero-order-holder (ZOH), its discrete transfer function is [9]

$$P_f(z) = (1 - z^{-1})\mathcal{Z}\left[\mathcal{L}^{-1}\left(\frac{P_f(s)}{s}\right)\right] \tag{3}$$

Therefore, the overall system can be treated as a discrete-time system and it is preferable to perform the design in the discrete-time domain.

Since the plant is modeled in the summation of the transfer functions for each resonance modes, the discrete transfer function can be obtained by taking Z-transform for each resonance modes and then summing them together. For simple illustration, the discrete transfer function for single resonance mode is given here. Define

$$P_i(s) = K_p \frac{(2 - T_d s)}{(2 + T_d s)} \frac{k_i}{(s^2 + 2\zeta_i\omega_i s + \omega_i^2)} \tag{4}$$

The discrete transfer function of $P_i(s)$ is can then be obtained in the form as

$$P_i(z) = \frac{b_{i1}z^{-1} + b_{i2}z^{-2} + b_{i3}z^{-3}}{1 + a_{i1}z^{-1} + a_{i2}z^{-2} + a_{i3}z^{-3}} \tag{5}$$

Accordingly, the parameters in eq. (5) can be calculated as

$$\begin{aligned} a_{i1} &= -e^{-\frac{2}{T_d}T_s} - 2e^{-\zeta_i\omega_i T_s}\cos(\omega_i\sqrt{1-\zeta_i^2}T_s) \\ a_{i2} &= e^{-2\zeta_i\omega_i T_s} + 2e^{-\frac{2}{T_d}T_s - \zeta_i\omega_i T_s}\cos(\omega_i\sqrt{1-\zeta_i^2}T_s) \\ a_{i3} &= -e^{-\frac{2}{T_d}T_s - \zeta_i\omega_i T_s} \end{aligned}$$

Define $\alpha_1 = e^{-\zeta_i\omega_i T_s}$, $\alpha_2 = \cos(\omega_i\sqrt{1-\zeta_i^2}T_s)$, which can be computed by $\alpha_1 = -a_{i3}/e^{-\frac{2}{T_d}T_s}$, $\alpha_2 = -(a_{i1} + e^{-\frac{2}{T_d}T_s})/2\alpha_1$. The damping ratio and natural frequency are ready to be obtained by

$$\zeta_i = 1/\sqrt{[\frac{\arccos(\alpha_2)}{\ln(\alpha_1)}]^2 + 1} \tag{6}$$

$$\omega_i = -\frac{\ln(\alpha_1)}{\zeta_i T_s} \tag{7}$$

The on-line identifier $\hat{N}(z)$ is activated when the nominal controller fails to maintain required tracking accuracy. On the other hand, as soon as the approximation error enters into the dead-zone and stay within it thereafter, the identification loop will be de-activated while the uncertain resonance mode is ready to be extracted according to the relationship given by (6) and (7). The identification loop is then replaced by a linear peak filter which takes the form

$$C_{pf}(z) = \frac{(z-1)(\alpha z + \beta)}{z^2 - 2e^{-\zeta_0\omega_0 T_s}\cos(\omega_0\sqrt{1-\zeta_0^2}T_s)z + e^{-2\zeta_0\omega_0 T_s}} \tag{8}$$

where $0 \le \zeta_0 \le 0.707$ is the damping ratio and ω_0 is the natural frequency of the peak filter, one zero at 1 is to minimize the unwanted distortion in the loop shape outside the disturbance frequency, the other zero determined by α and β is to guarantee the closed-loop stability.

III. ADAPTIVE IDENTIFICATION OF UNCERTAIN RESONANCE

Assume that one single resonance mode is subject to variation. The discrete transfer function (3) can be expressed in ascending powers of z^{-1} as

$$\begin{aligned} P_f(z^{-1}) &= P_n(z^{-1}) + P_u(z^{-1}) \\ &= \frac{z^{-d}(b_1 + b_2 z^{-1} + \cdots + b_{m+1}z^{-m})}{1 + a_1 z^{-1} + \cdots + a_n z^{-n}} \end{aligned}$$

where $d = n - m \ge 0$ denotes the relative degree, $P_n(z^{-1})$ and $P_u(z^{-1})$ denote the known plant dynamics and uncertain dynamics respectively.

As shown in Fig. 1, $C(z)$ is the nominal controller and $\hat{N}(z)$ is used to identify the uncertain resonance mode adaptively [10]. Consider the track-following mode when $r(k) = 0$. Let $P_f(z^{-1}) = \frac{N_f(z^{-1})}{D_f(z^{-1})}$, $P_n(z^{-1}) = \frac{N_n(z^{-1})}{D_n(z^{-1})}$,

$P_u(z^{-1})=\frac{N_u(z^{-1})}{D_u(z^{-1})}$. The approximation error can be expressed as

$$\begin{aligned} e(k) &= [P_n(z^{-1}) + P_u(z^{-1})]u_n(k) + P_u(z^{-1})u_c(k) + d(k) \\ &= \frac{[N_n(z^{-1})D_u(z^{-1}) + N_u(z^{-1})D_n(z^{-1})]u_n(k)}{D_n(z^{-1})D_u(z^{-1})} \\ &\quad + \frac{N_u(z^{-1})D_n(z^{-1})u_c(k)}{D_n(z^{-1})D_u(z^{-1})} + d(k) \end{aligned} \tag{9}$$

where $d(k) = d_o(k) + n(k)$ is the combined disturbance. Define

$$\begin{aligned} A(z^{-1}) &= D_n D_u = D_f(z^{-1}) = 1 + a_1 z^{-1} + ... + a_n z^{-n} \\ z^{-d}B(z^{-1}) &= N_n D_u + N_u D_n = N_f(z^{-1}) \\ &= z^{-d}(b_1 + b_2 z^{-1} + ... + b_{m+1} z^{-m}) \\ z^{-d_1}C(z^{-1}) &= N_u D_n = z^{-d_1}(c_1 + c_2 z^{-1} + ... + c_{l+1} z^{-l}) \end{aligned}$$

Then eq. (9) can be re-written as

$$\begin{aligned} A(z^{-1})e(k) &= z^{-d}B(z^{-1})u_n(k) + z^{-d_1}C(z^{-1})u_c(k) \\ &\quad + A(z^{-1})d(k) \end{aligned} \tag{10}$$

In this paper, we only consider the case when d=1 and d_1=1 to avoid the causality problem. Note that the condition d=1 and d_1=1 is common in discrete-time VCM models which are usually converted from the continuous models such as eq. (1) or eq. (2) using "ZOH" method. The results can be easily extended to $d\geq 2$, and $d\leq d_1$ can be guaranteed to avoid causality constraints under mild assumption [10]. Under the condition d=1 and d_1=1, it is ready to know that l=n−d_1.

For identification purpose, re-write eq. (10) in the linear regression form (ARX-model, [11]) as

$$e(k) = b_1\Big[u_n(k-d) - {\theta^*}^T\psi(k-d)\Big] + A(z^{-1})d(k)$$

where $\psi(k)$ is the regression vector and θ^* is the unknown parameter vector defined respectively by

$$\begin{aligned} \psi(k) &= [e(k), ..., e(k-n+1), u_n(k-1), ..., u_n(k-m), \\ &\quad u_c(k+d-d_1), ..., u_c(k+d-d_1-l)]^T \\ \theta^* &= [\frac{a_1}{b_1}, ..., \frac{a_n}{b_1}, -\frac{b_2}{b_1}, ..., -\frac{b_{m+1}}{b_1}, -\frac{c_1}{b_1}, ..., -\frac{c_{l+1}}{b_1}]^T \end{aligned}$$

Consider the adaptive control law

$$u_n(k-d) = \hat{\theta}^T(k-1)\psi(k-d)$$

with the adaptive parameter tuning low using the Normalized Least Mean Square (NLMS) algorithm [11] as

$$\hat{\theta}(k) = \hat{\theta}(k-1) + \frac{\mathrm{sgn}(b_1)\Gamma\psi(k-d)e(k)}{1+\beta\psi^T(k-d)\psi(k-d)} \tag{11}$$

where Γ is a positive definite matrix determining the updating rate and $\beta > 0$ is the normalizing constant.

Remark 1: Ideally the approximation error will converge to zero. Therefore, the control $u_n(k)$ becomes

$$\begin{aligned} u_n(k) &= -\frac{b_2}{b_1}u_n(k-1) - \cdots - \frac{b_{m+1}}{b_1}u_n(k-m) \\ &\quad - \frac{c_1}{b_1}u_c(k+d-d_1) - \cdots - \frac{c_{l+1}}{b_1}u_c(k+d-d_1-l) \end{aligned}$$

Note here d=d_1=1 and l=n−d_1, the discrete transfer function $N(z^{-1})$ can be obtained by

$$N(z^{-1}) = -\frac{c_1 + c_2 z^{-1} + \cdots + c_n z^{-(n-1)}}{b_1 + b_2 z^{-1} + \cdots + b_n z^{-(n-1)}} \tag{12}$$

which shows that $N(z)$ is realizable. For other possibilities of d and d_1, similar conclusion can be obtained.

In (11), the error between the measured PES and the estimated PES is used to determine the direction of parameter adaptation. However, the error $e(k)$ is always contaminated by the output disturbance, measurement noise, modeling errors, etc. Therefore, a series of robust modification is needed for the parameter identification algorithm. In fact, the functional approximation error defined by

$$\epsilon(k) \triangleq \hat{\theta}^T(k-1)\psi(k-d) - {\theta^*}^T\psi(k-d) \tag{13}$$

contributes partially to the error $e(k)$. Since $\epsilon(k)$ is supposed to drop down along the adaptation, its contribution to $e(k)$ will become less. When $\epsilon(k)$ drops down to certain level while at the same time the effect from various disturbances become dominant in $e(k)$, certain scheme need to be carried out to stop the adaptation. A dead zone augmented to the adaptation law can be one of the solutions. However, the size of $\epsilon(k)$ is usually unknown, the specified region to stop the adaptation should be carefully chosen to avoid instability. The dead-zone modification is then given by

$$\hat{\theta}(k) = \hat{\theta}(k-1) + \frac{\mu(k)\mathrm{sgn}(b_1)\Gamma\psi(k-d)e(k)}{1+\beta\psi^T(k-d)\psi(k-d)} \tag{14}$$

where

$$\mu(k) = \begin{cases} 1, & \text{if } |e(k)| \geq \delta \\ 0, & \text{otherwise} \end{cases}$$

with $\delta > 0$ being the threshold of the dead-zone.

The stability proof for the above scheme with dead-zone modification can be found in [10].

IV. SIMULATION STUDY

Consider a VCM actuator whose measured frequency response is plotted in Fig. 2 (solid line) and was modeled according to eq. (2) (dashed line). The parameters of the full model are: K_p=1.7686e6, T_d=1.0e−5, and the parameters for each resonance mode are given in Table I.

TABLE I
IDENTIFIED RESONANCE MODES

ζ_i	ω_i	k_i
0.4	2π50	1
0.02	2π8400	-1
0.015	2π15300	-1
0.01	2π18500	-1

In the simulation study, the servo sector number is 330, the spindle rotational speed is 7200 RPM, and therefore the sampling frequency is $330\cdot(7200/60)\approx$40kHz. The VCM actuator is subject to the input and output disturbances and

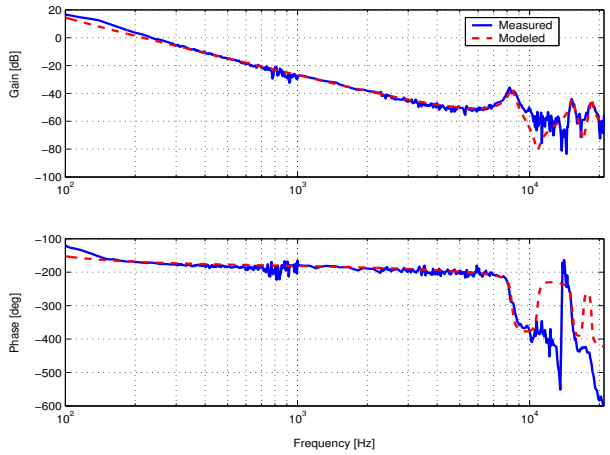

Fig. 2. Frequency response of VCM actuator.

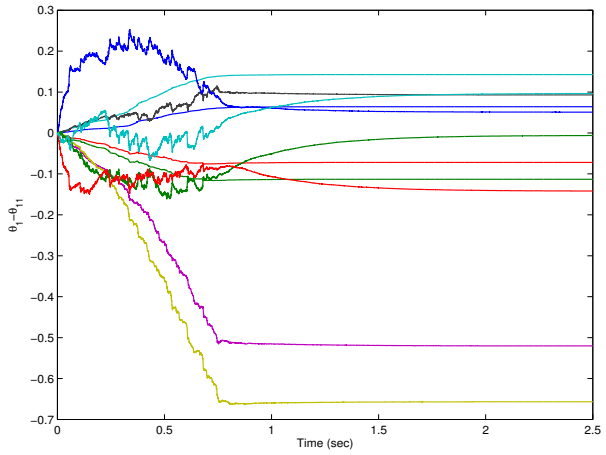

Fig. 3. Evolution of the parameter estimates.

measurement noise, which are obtained from a commercial drive [12].

The nominal controller is a PID control given by

$$C(z) = \frac{55.5247(z-0.9844)(z-0.9844)}{(z-1)(z-0.6242)}$$

A. Ideal case

Assume the resonance mode subject to variation is at 8.4kHz. For simplicity and illustration purpose only, we assume that the known resonance modes are well-compensated so that the nominal plant is a second order systems with the first rigid mode. Therefore, the system order $n = 4$, $m = 3$, the relative degree $d = d_1 = 1$. There are totally 11 unknown parameters to be identified. Different from [10], we assume that there is no external excitation such as the sinusoidal disturbance at single frequency except for white noise which is usually introduced for broadband excitation in adaptive control applications [13], and other input/output disturbances.

We first assume that the functional approximation error defined in (13) is available and can be used in the parameter adaptation. The initial conditions for adaptation are chosen as: $\hat{\theta}(0) = \mathbf{0}$, $\psi(0) = \mathbf{0}$. The adaptation gain matrix is $\Gamma = 7.9996e11 \cdot \mathbf{I}$ and the normalizing constant $\beta = 1$. The initial states of the full model plant $P_f(z)$, the known plant $P_n(z)$, the nominal controller $C(z)$, and the on-line identifier $\hat{N}(z)$ are all set to be zero. The reference signal is $r(k) = 0.0$ for track-following mode. Note that there will be no dead-zone for this ideal case. It is simulated when the resonance mode is subject to -10% variation, i.e., $f_2 = 7.56$kHz (-10%). The total simulation time is 600 revolutions, i.e., 4.95 seconds.

Fig. 3 shows the evolution of the parameter estimates for $f_2 = 7.56$kHz (-10%). The functional approximation error $\epsilon(k)$ during the adaptation are shown in Fig. 4. It can be seen that the parameter estimates converge at around 1.8 seconds and the functional approximation error $\epsilon(k)$ reaches its steady-state even earlier at around 1 second.

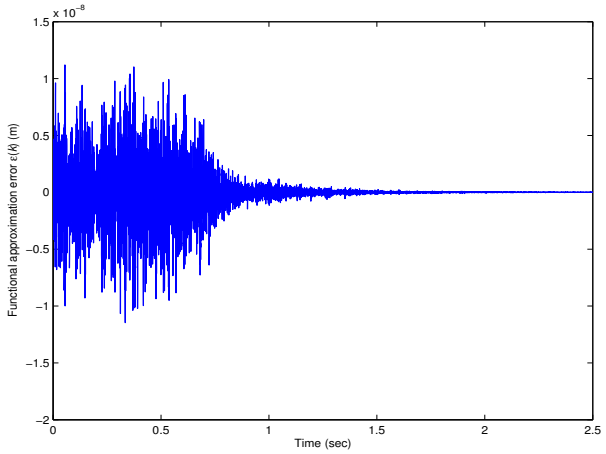

Fig. 4. Functional approximation error $\epsilon(k)$.

B. Practical case

However, the functional approximation error defined in (13) normally is not available. The only available signal in HDDs is the measured PES, which is always corrupted by various kind of disturbances/noise. Instead of the ideal functional approximation error (13), the error between the measured PES and the estimated PES (computed through the user-defined nominal plant) has to be used to determine the direction of parameter adaptation in practical application. However, the contribution from the parameter variation to the error signal would be hidden by various disturbances/noise. In other words, the error used for adaptation is dominated by various disturbances/noise rather than the functional approximation error. Therefore, it will make the identification extremely difficult. Additional signal processing by, for example, some band-pass filters is one of the solutions. But it will add extra computation burden to the microprocessor. In this paper, we adopt a practical method by setting the initial conditions of the on-line identifier to some nominal values rather than zero. The initial conditions are set in a way such that the functional approximation error is dominant in the overall PES signal rather than being hidden by various

disturbances/noise. The only effort to take is merely pre-storing some data and re-placement of the initial conditions. By doing so, the learning time is dramatically shortened while good identification performance is achieved. Therefore, it is a practical and easy for implementation.

The plant is the same as the one used for the ideal case, i.e., plant model $n = 4$, $m = 3$, and there are totally 11 unknown parameters to be identified. The plant is subject to the same input disturbance, output disturbance and sensor noise. The adaptation gain matrix is chosen as $\Gamma = 8.4e8 \cdot \mathbf{I}$ and the normalizing constant β=1. The initial regressor vector $\psi(0) = \mathbf{0}$. Fig. 5 and Fig. 6 plot the results when the nominal frequency subject to -10% variation, i.e., f_2=7.56kHz and ζ_2=0.006.

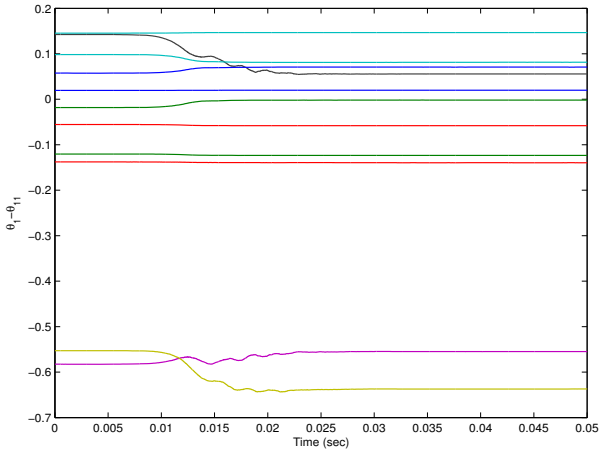

Fig. 5. Evolution of the parameter estimates.

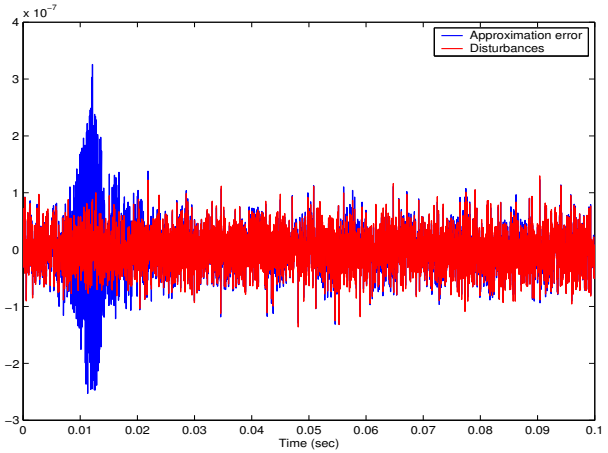

Fig. 6. Approximation error $e(k)$ and combined disturbances $d(k)$

As can be seen from Fig. 5, the parameter estimates converge at about 30 milli-seconds, which equivalent to around 4 revolutions. Compared to the ideal case, the learning/converging time is dramatically reduced. In addition, Fig. 6 shows that initially the approximation error drops down along the adaptation but stops dropping down further from around 30 milli-seconds onwards and stays in the steady-state at the same level as that of the combined disturbances. Therefore, the knowledge of the disturbance could be a reasonable guideline to determine the size of the dead zone.

C. Peak filter design

According to the identification results, the unknown resonance mode is ready to be extracted according to the relationship (6) and (7). Let us use the example when the nominal resonance frequency subject to -10% variation, i.e., f_2=7.56kHz. According to the identification results, the estimated resonance mode is centered at 7574Hz. As soon as the approximation error enters into the dead-zone and stays within it thereafter, at about 30 milli-seconds for this case, the identification loop can be cut off and replaced by a linear peak filter given by (8). Therefore, the natural frequency in (8) can be set as ω_0=2π7574. The choice of α and β will affect the stability as well as the resulting sensitivity function. According to the identification results, the peak filter is designed as

$$C_{pf}(z) = \frac{-0.21354(z-1)(z-0.2484)}{(z^2 - 0.6142z + 0.9875)}$$

The frequency responses of the open-loop system with the nominal control and the nominal control plus the add-on peak filter based on the identified resonance mode are plotted in Fig. 7, as well as the vector loci of the open-loop systems plotted in 8. The open-loop system achieves the crossover frequency f_c=1.07kHz, phase margin 45deg (red dot in Fig. 7), gain margin 11.35dB at 6.09kHz (red dot in Fig. 7). In addition, the second phase margin [14], [7] is 67deg at 7.3kHz, which provides a good stability margin to the variation of the resonance frequency and the peak of the gain. The phase at each resonance mode frequency is kept within a stable region of $\pm$90 deg (black dot in Fig. 7).

To illustrate the effectiveness of the adaptive design, we compare the sensitivity functions in Fig. 9, in which the black dashed curve shows the nominal design, the blue dashed curve shows the peak filter design without adaptation, and the red solid curve shows the peak filter design based on adaptive identification. It can be seen the peak filter design based on adaptive identification achieve the best performance, providing the best disturbance rejection 8dB gain attenuation at the resonance frequency without obvious distortion or sharp peak at other frequencies. The linear spectrum of PES is plotted in Fig. 10, which also shows the disturbance rejection of the designed peak filter.

V. CONCLUSION

An adaptive on-line scheme has been designed to identify the uncertain and varying resonance modes in HDD systems. The scheme did not require any extra excitation signal nor additional signal processing for the parameter identification. Compared to conventional method, the learning time has been greatly shortened as well as the converging time of the estimation error. Based on the identified results, the uncertain resonance mode can be extracted and a peak filter has been designed accordingly. The scheme has provided good stability margin at high frequency to the variation of

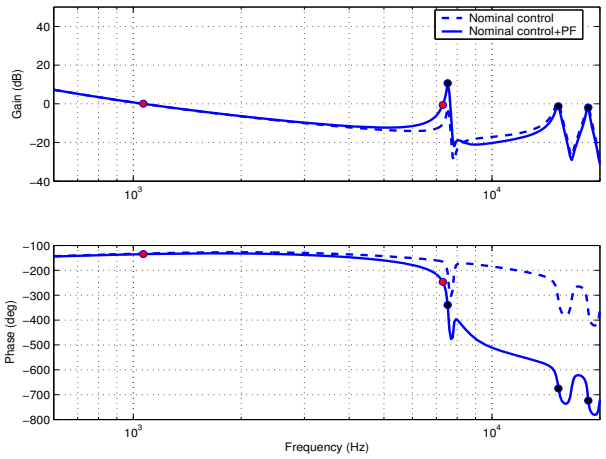

Fig. 7. Frequency response of open-loop system.

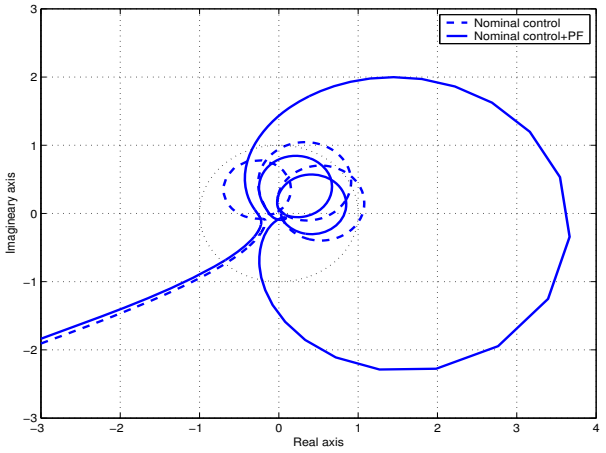

Fig. 8. Nyquist plot.

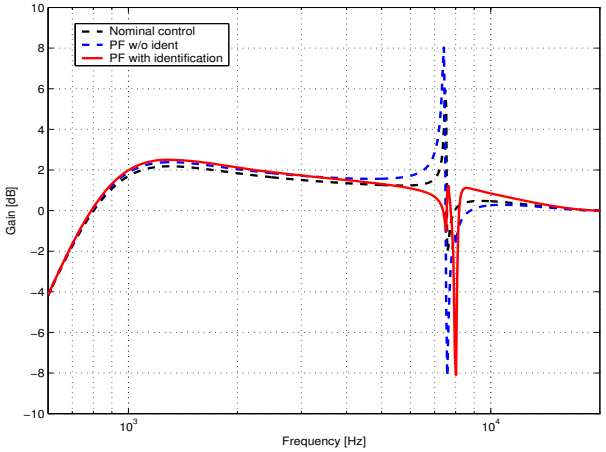

Fig. 9. Sensitivity magnitude of the closed-loop system.

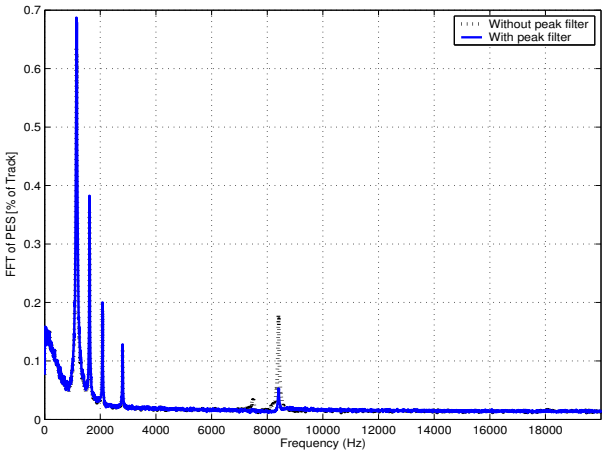

Fig. 10. Linear spectrum of PES.

the resonance frequency and the peak gain. Simulation results have shown the validity and effectiveness of the proposed scheme.

REFERENCES

[1] R. W. Wood and H. Takano, "Prospects for magnetic recording over the next 10 years," in *Proc. Int. Magn. Conf.*, San Diego, CA, 2006, CA-01, p. 98.

[2] D. Wu, G. Guo, and T.-C. Chong, "Adaptive compensation of microactuator resonance in hard disk drives," *IEEE Trans. Magn.*, vol. 36, no. 5, pp. 2247–2250, 2000.

[3] T. H. Yip, C. K. Tan, and Y. K. Kuan, "Behavior of spiral flow structures along the trailing edges of E-block arms under increasing airflow velocities," *IEEE Trans. Magn.*, vol. 42, no. 10, pp. 2591–2593, 2006.

[4] C. Du, L. Xie, and F. L. Lewis, "Using blending control to suppress multi-frequency disturbances," in *Proc. 10th Intl. Conf. on Control, Automation, Robotics and Vision*, Hanoi, Vietnam, 2008, pp. 1708–1713.

[5] C. I. Kang and C. H. Kim, "An adaptive notch filter for suppressing mechanical resonance in high track density disk drives," *Microsystem Technologies*, vol. 11, pp. 638–652, 2005.

[6] K. Ohno and T. Hara, "Adaptive resonance mode compensation for hard disk drives," *IEEE Trans. Ind. Electron.*, vol. 53, no. 2, pp. 624–630, 2006.

[7] M. Kobayashi, S. Nakagawa, and S. Nakamura, "A phase-stabilized servo controller for dual-stage actuators in hard disk drives," *IEEE Trans. Magn.*, vol. 39, no. 2, pp. 844–850, 2003.

[8] J. Zheng, G. Guo, Y. Wang, and W. E. Wong, "Optimal narrow-band disturbance filter for PZT-actuated head positioning control on a spinstand," *IEEE Trans. Magn.*, vol. 42, no. 11, pp. 3745–3751, 2006.

[9] G. F. Franklin, J. D. Powell, and A. Emami-Naeini, *Feedback Control of Dynamic Systemss*, 4th ed. Upper Saddle River, NJ: Prentice Hall, 2002.

[10] K. P. Tee, S. S. Ge, and E. H. Tay, "Adaptive resonance compensation for hard disk drive servo systems," in *Proc. 46th IEEE Conf. Decision and Control*, New Orleans, LA, 2007, pp. 3567–3572.

[11] L. Ljung, *System Identification: Theory for the User*, 2nd ed. Upper Saddle River, NJ: Prentice Hall, 1999.

[12] F. Hong, W. E. Wong, S. Zhang, and J. N. Teoh, "Servo performance analysis and pes prediction for patterned media technology," in *Digest of Asia-Pacific Magnetic Recording Conference*, Singapore, BQ-04, 2009.

[13] C. K. Pang, S. C. Tam, G. Guo, B. M. Chen, F. L. Lewis, T. H. Lee, and C. Du, "Improved disturbance rejection with online adaptive pole-zero compensation on a Φ-shaped PZT active suspension," *Submitted to Microsystem Technologies*, 2007.

[14] M. Kobayashi, S. Nakagawa, T. Atsumi, and T. Yamaguchi, "High-bandwidth servo control designs for magnetic disk drives," in *Proc. IEEE/ASME Int. Conf. Advanced Intelligent Mechatronics*, Como, Italy, 2001, pp. 1124–1129.